2014 American Control Conference (ACC)
June 4-6, 2014. Portland, Oregon, USA

Laser-based Guidance of a Quadrotor UAV for Precise Landing on an Inclined Surface

John Dougherty, Daewon Lee and Taeyoung Lee*

Abstract— **This paper is focused on measurement and control schemes for a quadrotor UAV to precisely land on a flat inclined surface without prior knowledge of the surface's orientation. Assuming that the location of the landing site is known, a quadrotor performs a flyover and uses lasers and a CMOS camera to detect the projections of the lasers on the ground plane to measure the relative ground plane angle of the landing site. This information is then used to design an aggressive landing trajectory such that the quadrotor touches down parallel to the landing surface. During the initial phase of the maneuver, a trajectory-tracking controller guides the quadrotor, and as it nears the landing phase, an attitude-tracking controller ensures that the attitude of the quadrotor matches the slope of the landing platform upon touchdown. This approach is illustrated by numerical examples and preliminary experimental results for laser-based surface angle determination.**

I. Introduction

A. Motivation and Background

Autonomous landing on an inclined surface is necessary for landing UAVs on boats in rough waters or for operation in unknown environments where an uninclined landing site may not be available [1], [2]. For the former case, a ship may have a flat landing platform, but its orientation is unsteady with time. A quadrotor should be able to measure the inclination as it changes with time and perform a landing maneuver safely. As for the latter case, it is essential that a quadrotor operating in uncertain terrain has some means of gathering information about its environment in order to touch down safely.

Das et al. outline an algorithm for landing a quadrotor UAV on an oscillating inclined surface using ultrasonic detection [3]. Ghadiok et al. propose a vision-based navigation system for a quadrotor capable of performing aggressive landing maneuvers on inclined surfaces using only onboard sensors [4].

Ultrasonic sensors are sensitive to the material of the targeted surface; in particular, ultrasonic sensors can give inaccurate readings for foam surfaces or other sound-absorbing materials. Infrared sensors are also often used for range finding purposes but can be inaccurate outdoors or in places with direct sunlight. Furthermore, the accuracy of these types of sensors tends to decrease when the relative angle of the targeted surface becomes large.

John Dougherty, Daewon Lee and Taeyoung Lee, Mechanical and Aerospace Engineering, George Washington University, Washington, DC 20052 {jadoc,daewonlee,tylee}@gwu.edu

*This research has been supported in part by NSF under the grants CMMI-1243000 (transferred from 1029551), CMMI-1335008, and CNS-1337722.

There are several drawbacks to vision-based feature detection approaches as well. It is often required that a specific pattern or marker that can be identified by a UAV is present at the landing site, such as a checker board [4], or an alphabet letter [5]. Thus, this approach requires the landing site to be predetermined, and the software must contain instructions on the type of feature or pattern designating a landing site. Therefore, it is not suitable for operations in unknown terrain. Additionally, the computational burden associated with many feature detection algorithms is high, meaning that the rate of data collection is low. This could result in a system that is too sluggish to track an oscillating surface incline or operate in real time.

B. Proposed Approach

In this paper, we propose a laser-based determination of the distance to and orientation of a landing site using low-cost laser modules and a CMOS camera. There are several desirable properties of the proposed laser-based measurement. Since the lasers are mounted to the quadrotor itself, no special patterns or markers are needed to designate a landing site, thereby making it suitable for operation in uncertain environments. This eliminates the need of predetermining a landing location; measurements can be taken during flight in real time. The proposed method implements image processing, but the computational load is relatively low since only bright points must be detected on the image plane.

The second part of this paper is focused on generating a safe landing trajectory for a given measurement of the landing surface orientation. Quadrotors are not able to softly and precisely land on inclined surfaces vertically since they are under-actuated. In order to safely land on an inclined surface, a trajectory should be designed such that the quadrotor's orientation matches the surface incline as it touches down. Aggressive perching has been demonstrated as open-loop maneuvers [6] and online parameter adaptation [7].

The landing trajectory presented in this paper is based on geometric nonlinear control systems for quadrotor UAVs [8], [9], [10]. First, a position tracking controller guides the quadrotor to the determined landing site, and, as it nears the landing phase, an attitude-tracking controller is engaged to align the attitude of the quadrotor to the landing surface. The entire hybrid trajectory is parameterized by the switching conditions, which are determined to meet boundary conditions for landing. The proposed approach addresses the guidance and control problems simultaneously, and it is developed in a coordinate-free fashion such that it can be uniformly applied to aggressive landing maneuvers.

978-1-4799-3274-0/$31.00 ©2014 AACC

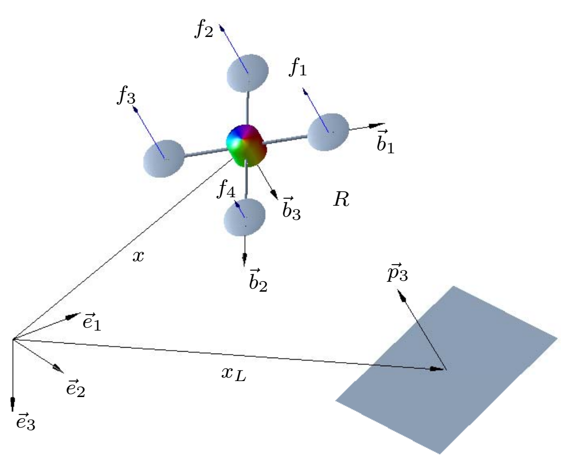

Fig. 1. Quadrotor model with an inclined landing surface

II. Problem Formulation

A. Quadrotor Dynamic Model

Consider a quadrotor UAV model illustrated in Fig. 1 [9]. This is a system of four identical rotors and propellers located at the vertices of a square, which generate a thrust and torque normal to the plane of this square. We choose an inertial reference frame $\{\vec{e}_1, \vec{e}_2, \vec{e}_3\}$ and a body-fixed frame $\{\vec{b}_1, \vec{b}_2, \vec{b}_3\}$. The origin of the body-fixed frame is located at the center of mass of this vehicle. The first and the second axes of the body-fixed frame, $\vec{b}_1, \vec{b}_2$, lie in the plane defined by the centers of the four rotors.

The configuration of this quadrotor UAV is defined by the location of the center of mass and the attitude with respect to the inertial frame. Therefore, the configuration manifold is the special Euclidean group $\mathsf{SE}(3)$, which is the semidirect product of $\mathbb{R}^3$ and the special orthogonal group $\mathsf{SO}(3) = \{R \in \mathbb{R}^{3\times 3} \,|\, R^T R = I, \det R = 1\}$.

The mass and the inertial matrix of a quadrotor UAV are denoted by $m \in \mathbb{R}$ and $J \in \mathbb{R}^{3\times 3}$. Its attitude, angular velocity, position, and velocity are defined by $R \in \mathsf{SO}(3)$, $\Omega, x, v \in \mathbb{R}^3$, respectively, where the rotation matrix R represents the linear transformation of a vector from the body-fixed frame to the inertial frame and the angular velocity Ω is represented with respect to the body-fixed frame. The distance between the center of mass to the center of each rotor is $d \in \mathbb{R}$, and the i-th rotor generates a thrust f_i and a reaction torque τ_i along $-\vec{b}_3$ for $1 \leq i \leq 4$. The magnitude of the total thrust and the total moment in the body-fixed frame are denoted by $f, M \in \mathbb{R}^3$, respectively.

The following conventions are assumed for the rotors and propellers, and the thrust and moment that they exert on the quadrotor UAV. We assume that the thrust of each propeller is directly controlled, and the direction of the thrust of each propeller is normal to the quadrotor plane. The first and third propellers are assumed to generate a thrust along the direction of $-\vec{b}_3$ when rotating clockwise; the second and fourth propellers are assumed to generate a thrust along the same direction of $-\vec{b}_3$ when rotating counterclockwise. Thus, the thrust magnitude is $f = \sum_{i=1}^4 f_i$, and it is positive when the total thrust vector acts along $-\vec{b}_3$, and it is negative when the total thrust vector acts along $\vec{b}_3$. By the definition of the rotation matrix $R \in \mathsf{SO}(3)$, the direction of the i-th body-fixed axis $\vec{b}_i$ is given by Re_i in the inertial frame, where $e_1 = [1; 0; 0], e_2 = [0; 1; 0], e_3 = [0; 0; 1] \in \mathbb{R}^3$.

Therefore, the total thrust vector is given by $-fRe_3 \in \mathbb{R}^3$ in the inertial frame. We also assume that the torque generated by each propeller is directly proportional to its thrust. Since it is assumed that the first and the third propellers rotate clockwise and the second and the fourth propellers rotate counterclockwise to generate a positive thrust along the direction of $-\vec{b}_3$, the torque generated by the i-th propeller about $\vec{b}_3$ can be written as $\tau_i = (-1)^i c_{\tau f} f_i$ for a fixed constant $c_{\tau f}$. All of these assumptions are fairly common in many quadrotor control systems [11], [12]. Then, the thrust of each propeller f_1, f_2, f_3, f_4 is directly converted into f and M, or vice versa. As such, the thrust magnitude $f \in \mathbb{R}$ and the moment vector $M \in \mathbb{R}^3$ are viewed as control inputs throughout this paper.

The equations of motion are given by

$$\dot{x} = v, \tag{1}$$

$$m\dot{v} = mge_3 - fRe_3 + \Delta_x, \tag{2}$$

$$\dot{R} = R\hat{\Omega}, \tag{3}$$

$$J\dot{\Omega} + \Omega \times J\Omega = M + \Delta_R, \tag{4}$$

where the *hat map* $\hat{\cdot} : \mathbb{R}^3 \to \mathfrak{so}(3)$ is defined by the condition that $\hat{x}y = x \times y$ for all $x, y \in \mathbb{R}^3$.

This identifies the Lie algebra $\mathfrak{so}(3)$ with $\mathbb{R}^3$ using the vector cross product in $\mathbb{R}^3$. The inverse of the hat map is denoted by the *vee* map, $\vee : \mathfrak{so}(3) \to \mathbb{R}^3$. Unstructured, but fixed uncertainties in the translational dynamics and the rotational dynamics of a quadrotor UAV are denoted by Δ_x and $\Delta_R \in \mathbb{R}^3$, respectively.

B. Precise Landing on an Inclined Surface

It is assumed that the position and the attitude of the quadrotor UAV can be measured from onboard or external sensors, such as GPS, Motion Capture cameras, or inertial measurement units. Suppose that the landing site is a flat surface without any feature or mark, and it is sufficiently large for landing of a given quadrotor UAV. Let $x_L \in \mathbb{R}^3$ be the location of the landing point. It is assumed that the first two components of x_L representing the horizontal position of the landing point are known. The third component of x_L describing the altitude of the landing point is unknown, but its range is available. The inclination of the landing site, defined by the unit-vector $\vec{p}_3$ that is normal to the landing surface, is also unavailable priorly. In short, only the horizontal position of the landing point is given.

The inclination of the landing surface and the altitude of the landing point should be determined during flight using onboard sensors, and based on those measurements, a safe landing trajectory should be designed. To achieve this goal, the following landing sequences are proposed in this paper:

(i) Measurement of landing surface inclination: at this first step, the quadrotor UAV is translated to a point that is

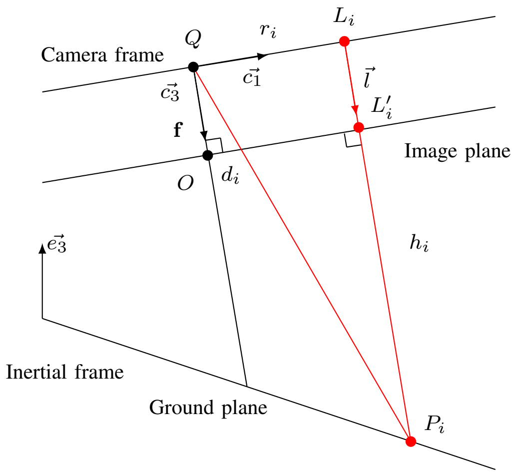

Fig. 2. Geometry of laser and camera using the pinhole camera model.

directly above the landing point. While hovering at the fixed point, the inclination of the landing surface and its altitude are measured from laser-based onboard sensors. The altitude of the hovering point is chosen such that it is sufficiently high to avoid any interference with the surface, but it is in the range of sensor capability.

(ii) Design of landing trajectory: this is to determine a landing trajectory from the hovering point at Step (i) to the landing point x_L, based on the measured surface inclination and altitude. A hybrid landing trajectory is designed such that the quadrotor lands at the desired landing point with zero velocity while aligning its attitude to the inclined landing surface.

The next two sections describe each of the above landing sequences more explicitly.

III. Laser-based Determination of Landing Surface

A system of laser modules are installed beneath a quadrotor UAV, and the corresponding bright points reflected on the landing surface are detected by a CMOS camera. By finding the coordinates of those points in the image plane, the altitude of each laser module can be determined, which yields the orientation of and distance to the landing surface relative to the quadrotor.

In this section, the central idea is illustrated by determining the altitude of a single point, and it is generalized for measurement for landing surface inclination.

A. Altitude Determination of a Single Point

Consider a camera fixed beneath a quadrotor, as illustrated at Fig. 2. Define a camera frame $\{\vec{c}_1, \vec{c}_2, \vec{c}_3\}$ such that each axis $\vec{c}_i$ is parallel to the body-fixed axis $\vec{b}_i$ and its origin is located at the focal point of the camera. It is assumed that the optical axis of the camera coincides with $\vec{c}_3$.

Using the pinhole camera model, the image plane is parallel to the $\vec{c}_1$-$\vec{c}_2$ plane and offset from the aperture along $\vec{c}_3$ by the focal length $\mathbf{f}$, and the origin of the image plane O is located at the intersection of the optical axis and the image plane.

A laser is installed at point L_i that is offset from the camera by some distance, r_i, along $\vec{c}_1$ and pointing downward, and the direction of the laser is given by $\vec{l}$ such that $\|\vec{l}\| = 1$ and $\vec{l} \parallel \vec{c}_3$. Let L_i' be the projection of L_i along $\vec{l}$ to the image plane. The laser beam intersects the ground plane at a point P_i, which is detected by the camera and appears in the image plane.

Let $d_i \in \mathbb{R}$ be the distance between the projection of the laser in the image plane and O and obtained through image processing, and let $h_i \in \mathbb{R}$ be the distance between L_i' and P_i. Using similar triangles, the measurement d_i is related to h_i as

$$h_i = \mathbf{f}\left(\frac{r_i - d_i}{d_i}\right). \tag{5}$$

In short, the distance between the image plane and the ground along the direction of the optical axis can be determined by measuring the distance to the projection of the laser in the image plane. When the image plane is normal to $\vec{e}_3$, e.g. hovering case, h_i corresponds to the altitude of the point L_i'. If the image plane is not parallel, the attitude of the quadrotor can be used along with information about the surface inclination to project h_i along the vertical direction to obtain the altitude of the point, which is discussed in the following section.

B. Surface Incline Determination

For an inclined ground plane, two lasers along the same axis can yield the relative angle between the axis and ground plane. Three or more lasers defining a plane can be used to find the 3D orientation of the ground plane with respect to the quadrotor. First consider two lasers at points L_1 and L_2 lying along $\vec{c}_1$, with their offsets given as r_1 and r_2, respectively, and their directions given by $\vec{l}$. Note that L_1 lies along $\vec{c}_1$, and L_2 lies along $-\vec{c}_1$, as shown in Fig. 3. The projected altitudes along $\vec{l}$ of each point L_i' can be obtained using (5), and these altitudes can be used to find the distance between O and O' in Fig. 3:

$$h_{O,12} = \frac{h_1 - h_2}{r_1 + r_2} r_2 + h_2. \tag{6}$$

Let $\gamma \in \mathbb{R}$ be the relative angle of the image plane with respect to the ground plane. It can be written as

$$\gamma = \tan^{-1}\left(\frac{h_1 - h_2}{r_1 + r_2}\right). \tag{7}$$

Assuming that the attitude of the quadrotor, represented by the angle ϕ of the camera frame to the inertial frame, is available, the inclination α of the ground is obtained

$$\alpha = \gamma - \phi. \tag{8}$$

Also, the distance from Q to Q', namely the altitude of Q, can be expressed as:

$$H_{Q,12} = (h_{O,12} + \mathbf{f})(\cos\phi - \sin\phi \tan\alpha). \tag{9}$$

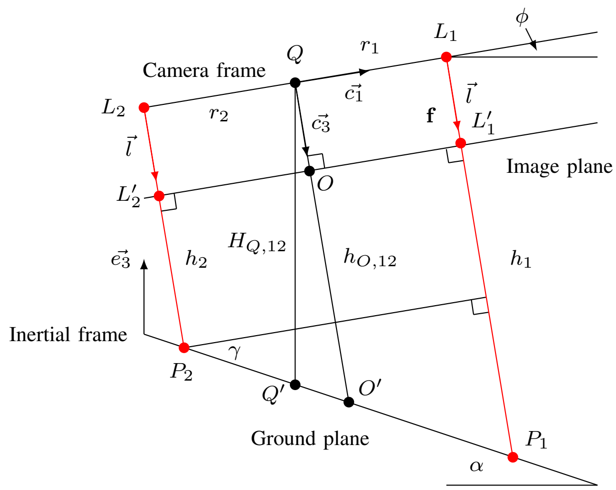

Fig. 3. Geometry of two lasers used to find relative ground plane angle.

These are repeated by using two additional lasers placed at points L_3 and L_4 along $\vec{c_2}$ to obtain the orientation of the landing surface in three-dimensional space.

IV. Design of Landing Trajectories

At the first stage of the proposed landing sequence, the quadrotor UAV is translated into a hovering position x_H that is directly above the landing point x_L, and the altitude and the inclination of the landing surface are measured using the laser-based determination scheme described at the previous section. By the completion of the first stage, the complete location of the landing point x_L including its altitude and the inclination of the landing surface described by the unit-vector $\vec{p}_3$ normal to the surface are available.

A. Quadrotor Tracking Controls

Since it is only possible to achieve asymptotic output tracking for at most four quadrotor UAV outputs, we define two flight modes, namely (1) an attitude controlled flight mode, and (2) a position controlled flight mode [8], [9], [10] and design control systems for each mode.

Geometric control systems with a generalized integral term to eliminate the effects of disturbances are summarized as follows (see [9] for detailed development).

a) Attitude Tracking Control: Suppose that a smooth attitude command $R_d(t) \in \mathsf{SO(3)}$ satisfying $\dot{R}_d = R_d\hat{\Omega}_d$ is given, where $\Omega_d(t)$ is the desired angular velocity, which is assumed to be uniformly bounded. An attitude error vector $e_R \in \mathbb{R}^3$, and an angular velocity error vector $e_\Omega \in \mathbb{R}^3$ are given by

$$e_R = \frac{1}{2}(R_d^T R - R^T R_d)^\vee, \quad e_\Omega = \Omega - R^T R_d \Omega_d, \tag{10}$$

A nonlinear controller for the attitude controlled flight mode is designed as

$$\begin{aligned} M = &-k_R e_R - k_\Omega e_\Omega - k_I e_I \\ &+ (R^T R_d \Omega_d)^\wedge J R^T R_d \Omega_d + J R^T R_d \dot{\Omega}_d, \end{aligned} \tag{11}$$

$$e_I = \int_0^t e_\Omega(\tau) + c_2 e_R(\tau) d\tau, \tag{12}$$

where k_R, k_Ω, k_I, c_2 are positive constants, and the total thrust f can be arbitrarily chosen. The corresponding stability properties are summarized as follows.

Proposition 1: [9] Consider the control moment M defined in (11)-(12). If c_2 is sufficiently small, then the equilibrium of the zero attitude tracking errors $(e_R, e_\Omega, e_I) = (0, 0, \frac{\Delta_R}{k_I})$ is almost globally asymptotically stable with respect to e_R and e_Ω[1], and the integral term e_I is globally uniformly bounded. It is also locally exponentially stable with respect to e_R and e_Ω.

b) Position Tracking Control: Suppose that an arbitrary smooth position tracking command $x_d(t) \in \mathbb{R}^3$ is given. The position tracking errors for the position and the velocity are given by:

$$e_x = x - x_d, \quad e_v = \dot{e}_x = v - \dot{x}_d. \tag{13}$$

Similar with (12), an integral control term for the position tracking controller is defined as

$$e_i = \int_0^t e_v(\tau) + c_1 e_x(\tau) d\tau, \tag{14}$$

for a positive constant c_1. The desired attitude of the position controlled tracking mode is defined as

$$R_c = [b_{1_c};\, b_{3_c} \times b_{1_c};\, b_{3_c}], \quad \hat{\Omega}_c = R_c^T \dot{R}_c, \tag{15}$$

where $b_{3_c} \in \mathsf{S}^2$ is given by

$$b_{3_c} = -\frac{-k_x e_x - k_v e_v - k_i \mathrm{sat}_\sigma(e_i) - mge_3 + m\ddot{x}_d}{\|-k_x e_x - k_v e_v - k_i \mathrm{sat}_\sigma(e_i) - mge_3 + m\ddot{x}_d\|}, \tag{16}$$

for positive constants k_x, k_v, k_i, σ. The unit vector $b_{1_c} \in \mathsf{S}^2$ is selected to be orthogonal to b_{3_c}, thereby guaranteeing that $R_c \in \mathsf{SO(3)}$. It can be chosen to specify the desired heading direction. The attitude error and the angular velocity error are defined as (10) using R_c and Ω_c.

A nonlinear controller for the position tracking control mode is designed as

$$f = (k_x e_x + k_v e_v + k_i \mathrm{sat}_\sigma(e_i) + mge_3 - m\ddot{x}_d) \cdot Re_3, \tag{17}$$

$$\begin{aligned} M = &-k_R e_R - k_\Omega e_\Omega - k_I e_I \\ &+ (R^T R_c \Omega_c)^\wedge J R^T R_c \Omega_c + J R^T R_c \dot{\Omega}_c. \end{aligned} \tag{18}$$

The corresponding stability properties are summarized as follows:

Proposition 2: [9] Consider the control system defined by (17) and (18). The controller parameters can be chosen such that the zero equilibrium of the tracking errors is exponentially stable with respect to e_x, e_v, e_R, e_Ω, and it is almost globally attractive. The integral terms e_i, e_I are uniformly bounded.

[1] see [13, Chapter 4] for the definition of partial stability

B. Hybrid Landing Trajectories

Due to the almost global stability properties, the control system is robust to switching conditions. The position and the velocity of the quadrotor at the switching instant are defined as $x_S \in \mathbb{R}^3$ and $v_S \in \mathbb{R}^3$, respectively. Let $t = 0$ at the beginning of the landing maneuver, and let t_S and t_L be the time of switching and landing, respectively.

Suppose that t_S, t_L are prescribed and fixed. We define the landing trajectory in terms of x_S and v_S as follows. As the quadrotor is hovering at the beginning of the landing maneuver, the initial conditions are given by

$$x(0) = x_H,\ v(0) = 0_{3\times 1},\ R(0) = I_{3\times 3},\ \Omega(0) = 0_{3\times 1}. \tag{19}$$

For the given switching condition, we also have $x(t_S) = x_S, \quad v(t_S) = v_S$. The desired landing trajectory satisfying these boundary conditions can be parameterized by t as follows. For $1 \leq i \leq 3$, its i-th component is given by

$$\begin{aligned} x_{d_i}(t) &= (v_{S_i} t_S + 3(x_{H_i} - x_{S_i}))\frac{t^4}{t_S^4} \\ &\quad - (v_{S_i} t_S + 4(x_{H_i} - x_{S_i}))\frac{t^3}{t_S^3} + x_{H_i}. \end{aligned} \tag{20}$$

The desired direction of the first body-fixed axis is chosen such that it is normal to the vertical axis:

$$b_{1_c} = \frac{e_3 \times p_3}{\|e_3 \times p_3\|}. \tag{21}$$

Substituting x_d and b_{1_c} into the position tracking controller (17) and (18), we numerically simulate the controlled system from the initial condition (19) until $t = t_S$ to obtain $(x(t), v(t), R(t), \Omega(t))$ for $0 \leq t \leq t_S$.

Next, when $t > t_S$, the attitude tracking controller is engaged, where the desired attitude and the desired angular velocity are chosen as

$$R_d(t) = \begin{bmatrix} b_{1_c}, & b_{1_c} \times p_3, & -p_3 \end{bmatrix}, \quad \Omega_d(t) = 0_{3\times 1}. \tag{22}$$

Note that together with (21), the above definition guarantees that $R_d(t)$ is a rotation matrix in $\mathsf{SO}(3)$. The total thrust f is also selected. Substituting these into (10)–(12), we simulate the controlled system from the initial condition $(x(t_S), v(t_S), R(t_S), \Omega(t_S))$ for $t_S \leq t \leq t_L$.

In short, the complete landing trajectory is described in terms of the switching position x_S, the switching velocity v_S, and the total thrust f of the attitude tracking mode. Using these, the problem of designing landing trajectory is converted into a nonlinear equation to find x_S, v_S, and f such that $x(t_L) = x_L$. The other terminal boundary condition to align the attitude of the quadrotor to the landing surface is not explicitly imposed as a constraint based on the assumption that $t_L - t_S$ is sufficiently large: the error of the attitude tracking controller is converged to zero before $t = t_L$. This is not a restrictive assumption, as the attitude dynamics of controlled quadrotors are relatively fast.

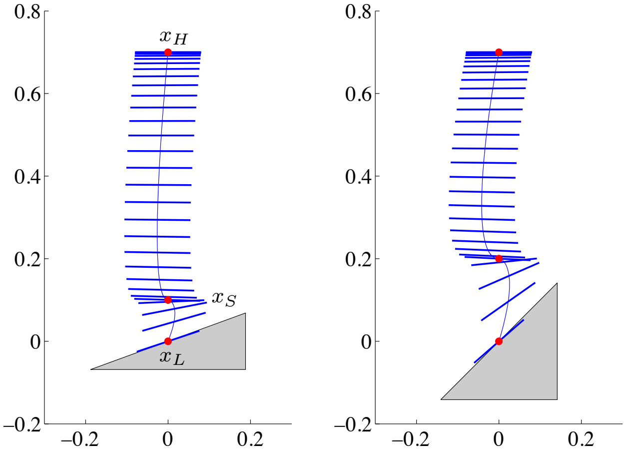

Fig. 4. Snapshots of landing trajectories for $\alpha = 20°$ and $\alpha = 45°$

C. Numerical Examples

Consider a quadrotor UAV with $m = 1.22\,\mathrm{kg}$ and $J = \mathrm{diag}[0.55,\, 0.55,\, 1.05] \times 10^{-2}\,\mathrm{kgm}^2$. The hovering point and the landing point are selected as $x_H = [0,\, 0,\, 0.7]^T\,\mathrm{m}$ and $x_L = 0_{3\times 1}$, respectively. For given $t_S = 2\,\mathrm{sec}$ and $t_L = 2.3\,\mathrm{sec}$, the switching point x_S, the switching velocity v_S, and the total thrust are numerically obtained to satisfy x_L.

As this problem is underdetermined, one may consider optimizing the parameters with respect to a certain cost function. Instead, here we specify the following additional constraints: the switching point x_S is on the line joining the hovering point x_H and the landing point x_L, and the velocity at the switching point is horizontal, i.e., $v_S^T e_3 = 0$.

The snapshots that illustrate the resulting position and attitude maneuvers of the quadrotor UAV are shown at Fig. 4 for two landing surface inclinations.

V. Preliminary Experimental Results

A. Hardware Configuration

The quadrotor is assembled from a Turnigy Talon V2 carbon fiber frame with a 550 mm span and can be seen in Fig. 5(a). A Point Grey Research Firefly MV Mono camera with a 4 mm lens is rigidly mounted underneath the bottom center plate by a custom 3D printed ABS plastic mount, shown in Fig. 5(c). For preliminary testing, the camera is linked to a host computer via USB for image processing in OpenCV at a rate of approximately 40 fps.

Eight 650 nm 5mW Instapark laser modules are mounted to the frame by custom 3D printed ABS plastic mounts in such a way as to maximize the distance between them while having each group of four exit the field of view of the camera at approximately the same altitude. This laser configuration can be seen in Fig. 5(b). The precise offset distance of each laser must be found through calibration by taking measurements at a known altitude, attitude, and surface inclination before flight for accurate results. For the experimental results given in the following section, the laser offset distances $\{r_1, r_2, ..., r_8\}$ were determined to be

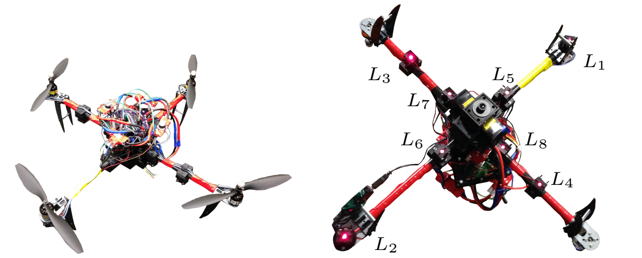

(a) Custom-built quadrotor UAV.

(b) View of underside of quadrotor with laser modules exposed.

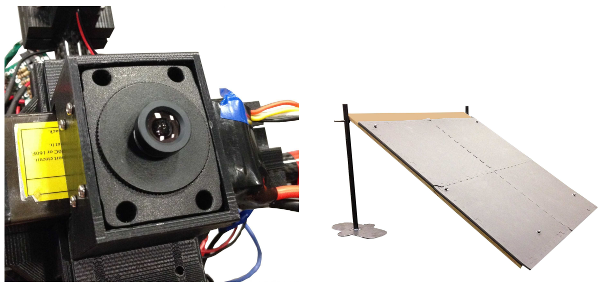

(c) CMOS camera mounted beneath quadrotor.

(d) Custom-built $4' \times 4'$ landing platform with adjustable inclination.

Fig. 5. Hardware configuration of quadrotor with detailed view of camera and laser mounts along with photograph of landing platform used in experiments.

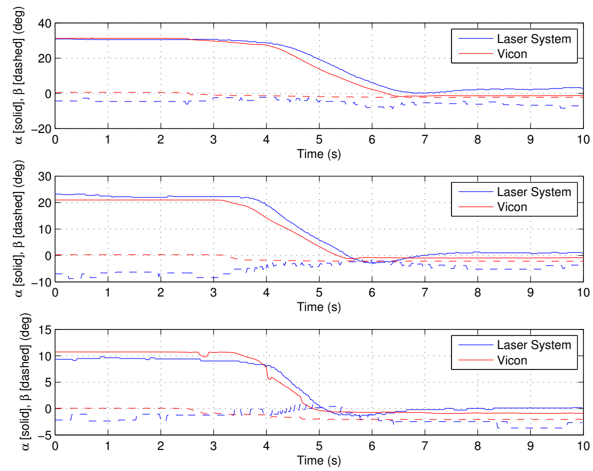

Fig. 6. Inclined surface with $\alpha = \{31, 21, 11\}$ degrees and $\beta = 0$, where α and β are the relative inclinations along $\vec{b_1}$ and $\vec{b_2}$, respectively. α is designated by solid lines; β is designated by dashed lines. Quadrotor was held in place over the landing surface for data collection.

$\{0.3194, 0.2530, 0.1444, 0.1642, 0.1020, 0.0903, 0.0746, 0.0683\}$ m.

B. Laser System Tests

Preliminary experiments were carried out by manually holding the quadrotor in place, in order to characterize the performance of the laser-based vision system and its accuracy in determining the incline of a flat landing surface for several inclinations. The quadrotor is held flat over a landing platform, shown in Fig. 5(d), that can be adjusted between 0 and 31 ± 0.5 degrees of inclination by means of one pivoting end while Vicon markers track its exact orientation. Data collection begins with the landing surface at some inclination, and after a few seconds the surface is manually lifted to zero inclination. Results of these experiments are given in Fig. 6.

Overall, the laser system gives reasonable estimates of the ground inclination suitable for use in designing a landing trajectory. During the transition to zero incline, the system is able to track the surface angle quite well. Thus, this method shows promise for being used to measure the inclination of a surface that is changing with time, such as in the case of a ship.

VI. Conclusions

This paper considers a new type of low-cost onboard sensing used along with a nonlinear hybrid control approach to aid a quadrotor UAV in landing on an unknown, inclined surface. Future work includes the formulation of this problem completely in three dimensions to avoid restrictive assumptions along with the development of an estimation scheme to incorporate stochastic properties of measurement uncertainties to improve accuracies. Furthermore, the problem of designing an adaptive landing trajectory for time-varying surface inclinations should be addressed.

References

[1] J. Moore, "A system for landing an autonomous radio controlled helicopter on sloped terrain," Master's thesis, MIT, 1994.
[2] S. Oh, K. Pathak, S. Agrawal, H. Pota, and M. Garratt, "Approaches for a tether-guided landing of an autonomous helicopter," *IEEE Transactions on Robotics*, vol. 22, no. 3, pp. 536–544, 22006.
[3] P. Das, S. Swami, and J. Conrad, "An algorithm for landing a quadrotor unmanned aerial vehicle on an oscillating surface," in *Proceedings on the IEEE Southeastcon*, 2012.
[4] V. Ghadiok, J. Goldin, and W. Ren, "On the design and development of attitude stabilization, vision-based navigation, and aerial gripping for a low-cost quadrotor," *Autonomous Robots*, vol. 33, pp. 41–68, 2012.
[5] D. Lee, T. Ryan, and H. Kim, "Autonomous landing of a VTOL UAV on a moving platform using image-based visual servoing," in *Proceedings of the IEEE International Conference on Robotics and Automation*, 2012.
[6] S. Bayraktar and E. Feron, "Experiments with small helicopter automated landings at unusual attitudes," arXiv, 2008. [Online]. Available: http://arxiv.org/abs/0709.1744
[7] D. Mellinger, N. Michael, and V. Kumar, "Trajectory generation and control for precise aggressive maneuvers with quadrotors," *International Journal Of Robotics Research*, vol. 31, no. 5, pp. 664–674, 2012.
[8] T. Lee, M. Leok, and N. McClamroch, "Geometric tracking control of a quadrotor UAV on SE(3)," in *Proceedings of the IEEE Conference on Decision and Control*, 2010, pp. 5420–5425.
[9] F. Goodarzi, D. Lee, and T. Lee, "Geometric nonlinear PID control of a quadrotor UAV on $\mathsf{SE}(3)$," in *Proceedings of the European Control Conference*, Zurich, July 2013.
[10] T. Lee, M. Leok, and N. McClamroch, "Nonlinear robust tracking control of a quadrotor UAV on $\mathsf{SE}(3)$," *Asian Journal of Control*, vol. 15, no. 2, pp. 391–408, Mar. 2013.
[11] A. Tayebi and S. McGilvray, "Attitude stabilization of a VTOL quadrotor aircraft," *IEEE Transactions on Control System Technology*, vol. 14, no. 3, pp. 562–571, 2006.
[12] P. Castillo, R. Lozano, and A. Dzul, "Stabilization of a mini rotorcraft with four rotors," *IEEE Control System Magazine*, pp. 45–55, 2005.
[13] W. Haddad and V. Chellaboina, *Nonlinear Dynamical Systems and Control: A Lyapunov-Based Approach*. Princeton University Press, 2008.